Soil moisture modelling with ERA5-Land retrievals, topographic indices and in-situ measurements and its use for predicting ruts

Marian Schönauer[1], Anneli M. Ågren[2], Klaus Katzensteiner[3], Florian Hartsch[1], Paul Arp[4], Simon Drollinger[5], Dirk Jaeger[1]

[1]Department of Forest Work Science and Engineering, University of Göttingen, Göttingen, Germany
[2]Department of Forest Ecology and Management, Swedish University of Agricultural Sciences, Umeå, Sweden
[3]Institute of Forest Ecology, University of Natural Resources and Life Sciences, Vienna, Vienna, Austria
[4]Forestry and Environmental Management, University of New Brunswick, New Brunswick, Canada
[5]Department of Physical Geography, University of Göttingen, Göttingen, Germany

Correspondence to: Marian Schönauer (marian.schoenauer@uni-goettingen.de)

Abstract

Spatiotemporal modelling is an innovative way of predicting soil moisture and has promising applications in supporting sustainable forest operations. One such application is the prediction of rutting, since rutting can cause severe damage to forest soils and ecological functions.

In this work, we used ERA5-Land soil moisture retrievals and several topographic indices to model variations of in-situ soil water content, by means of a random forest model. We then correlated the predicted soil moisture with rut depth from different trials.

Our spatiotemporal modelling approach successfully predicted soil moisture with a Kendall's rank correlation coefficient of 0.62 (R^2 of 64%). The final model included the spatial depth-to-water index, topographic wetness index, stream power index, as well as temporal components such as month and season, and ERA5-Land soil moisture retrievals. These retrievals showed to be the most important predictor in the model, indicating a large temporal variation. The prediction of rut depth was also successful, resulting in a Kendall's correlation coefficient of 0.61.

Our results demonstrate that by using data from several sources, including ERA5-Land retrievals, topographic indices and in-situ soil moisture measurements, we can accurately predict soil moisture and use this information to predict rut depth. This has practical applications in reducing the impact of heavy machinery on forest soils and avoiding wet areas during forest operations.

Keywords: spatiotemporal modelling, forest management, forest engineering, rutting, downscaling, reanalysis

1 Introduction

For decades, forestry research has sought solutions to accurately predict the trafficability of forest soils (Murphy et al., 2007; White et al., 2012; Mattila and Tokola, 2019). In order to further sustainable forest management, efficient protection of forest soils is mandatory (Vega-Nieva et al., 2009; Uusitalo et al., 2019; Picchio et al., 2020). Heavy harvesting and forwarding machines have been frequently associated with severe soil damage, particularly when operating on soils with low bearing capacity (Horn et al., 2007; Allman et al., 2017). Soil compaction is a common consequence of harvesting operations (Eliasson, 2005; Ampoorter et al., 2010; DeArmond et al., 2021) and has shown to be detrimental to a number of ecological

functions, including soil biota (Beylich et al., 2010), hydrological patterns, and nutrient supply, with potential drawbacks on plant growth and site productivity (Curzon et al., 2022). In addition to soil compaction, machine traffic can also result in deep ruts (Horn et al., 2007; Poltorak et al., 2018; Ala-Ilomäki et al., 2021), which affect site hydrology and increase anaerobic conditions at the rut's base, where air-filled porosity is reduced, leading to minimized soil aeration (Hansson et al., 2019).

The risk of causing high degrees of soil compaction and rutting is mainly attributed to soil properties such as initial soil bulk density and texture, as well as the current soil water content (Cambi et al., 2015; Crawford et al., 2021). Moist soils show a higher susceptibility to damage since the internal friction is decreased through water embracing soil particles (Hillel, 1998), reducing the soil bearing capacity and the ability for elastic responses to machine-induced impacts (McNabb et al., 2001).

To support forestry management and machine operators, accurate cartographic information on soils with low bearing capacity is essential (Campbell et al., 2013; Jones and Arp, 2017; Sirén et al., 2019). However, existing models that rely on detailed soil maps to retrieve soil mechanical parameters (e.g. Grüll, 2011; Heubaum, 2015) require a high level of input data, and high-resolution soil maps are only available for selected areas, hindering their large-scale application (Vega-Nieva et al., 2009; Kristensen et al., 2019). Therefore, researchers have turned to topographic modelling as a more promising approach (White et al., 2012; Lidberg et al., 2020), as it requires only digital elevation models (DEM), which are increasingly available for most parts of Europe (Guo et al., 2017; Hoffmann et al., 2022). One topographic index that has been extensively studied is the "depth-to-water" (DTW) concept, originally developed and tested at the University of New Brunswick by Meng, Ogilvie, and Arp, as described by Murphy et al. (2007; 2009). The DTW concept calculates flow lines across areas of interest by determining a flow accumulation and selecting lines that originate at a set threshold of accumulated upstream contributing areas. Using a cost function that considers the cell-to-cell slopes, the vertical distances from each cell within a raster to the nearest simulated flow line are ascertained. DTW is well documented (e.g. Vega-Nieva et al., 2009; Murphy et al., 2011; White et al., 2012).

Previous research has shown that the DTW index performs relatively well in predicting wet areas in forested formerly glaciated landscapes compared to other indices (Ågren et al., 2014; Larson et al., 2022). Recent studies have explored further developments in moisture prediction by utilizing machine learning algorithms applied to a variety of freely available data and diverse retrieved information, including different topographic indices calculated on DEMs. Ågren et al. (2021) used 28 topographic predictor variables in an eXtreme Gradient Boosting model (Chen et al., 2021) to predict soil moisture across the entire Swedish forest landscape at high resolution (2x2 m). Although topographic modelling approaches are widely used, they often fail to adjust to seasonal changes in soil water regimes. Static maps may not adequately represent temporal occurrences of flow lines, wet fields, or water-saturated soils. To address this issue, the DTW concept offers a potential solution, enabling the calculation of different scenarios ranging from ‘very dry’ or ‘frozen’ to ‘wet’ soil conditions. However, selecting the most accurate DTW scenario requires high expertise (Leach et al., 2017; Lidberg et al., 2020), and mistakes can lead to reduced accuracy and result in potential soil damages that could be avoided.

Therefore, we believe that the next crucial step in soil moisture modelling is to incorporate a temporal component that enables the prediction of rasters for any given time and area. One approach to achieve this was designed by Schönauer et al. (2022), who developed a spatiotemporal prediction model. Dynamic satellite-based retrievals of soil moisture with coarse spatial resolution (Soil Moisture Active Passive Mission) were combined with high-resolution but static topographic maps. This resulted in improved performance in predicting moisture values across time-series conducted on sites in Finland, Germany, and Poland. The incorporation of a dynamic component into the prediction model enabled reflection of the current overall

moisture conditions on the study sites. This allowed to calculate daily prediction grids that could support forestry practice and enable the guidance of machine operators on sites to avoid traffic on wet areas susceptible to damages. However, a validation of predicting rut depth by models of this kind has not been facilitated yet.

The effectiveness of soil moisture modelling, whether based on static or dynamic independent variables, is ultimately constrained by the quality of the dependent variable, which in this case is in-situ soil moisture. Manual measurements of soil moisture have been conducted in numerous studies using different devices, such as hand-held time-domain reflectometry sensors (Kemppinen et al., 2018; Uusitalo et al., 2019) or impedance measuring techniques (e.g. Schönauer et al., 2021b). Despite the potential inaccuracies associated with these techniques (Walker et al., 2004; Francesca et al., 2010), they offer significant advantages in terms of flexibility, scalability, low investment costs, and minimal maintenance. Another option is the use of continuously measuring sensor networks (e.g. Oliveira et al., 2021), which can provide relatively reliable measurements but with limited spatial coverage due to the high costs of installation and maintenance.

In this study, we built upon the approach developed by Schönauer et al. (2022) by incorporating additional data sources, including additional topographic indices, soil maps, and soil moisture retrievals from ERA5-Land for two soil depths. The study also used two types of data sources for soil moisture measurements: manual measurements using a handheld moisture meter, and data from two continuously measuring sensor networks. We argue that manual measurements are simpler and can be applied to larger areas, while sensor networks are more expensive and limited to chosen positions.

The study had two main objectives: 1. to train soil moisture models using the two individual data sets (manual measurements and sensor networks) and evaluate their prediction performance, and 2. to select the best combination of predictor variables (e.g. topographic indices, ERA5-Land values) using a repeated cross-validation approach and compare the best models with rut depth data obtained during four trials using a forwarder.

2 Material and Methods

To model soil water content (SWC), random forest models were trained using two separate datasets: manual in-situ measurements using an impedance measuring technique (IMT) and continuously measuring soil sensor networks (SSN). To both datasets we added predictor variables derived from topographic indices (e.g. depth-to-water, topographic wetness index), soil maps, SWC estimates from the ERA5-Land campaign (SWC_{ERA}), and numerical values for date (month and season). We performed cross-validation and reduced features stepwise to choose the best-performing model. Subsequently, the two final models (for IMT and SSN) were used to predict SWC for the positions and dates of different field trials with a forwarder. During this field trials, rut depth data was captured, and compared to the predictions from the final SWC-models (Figure 1).

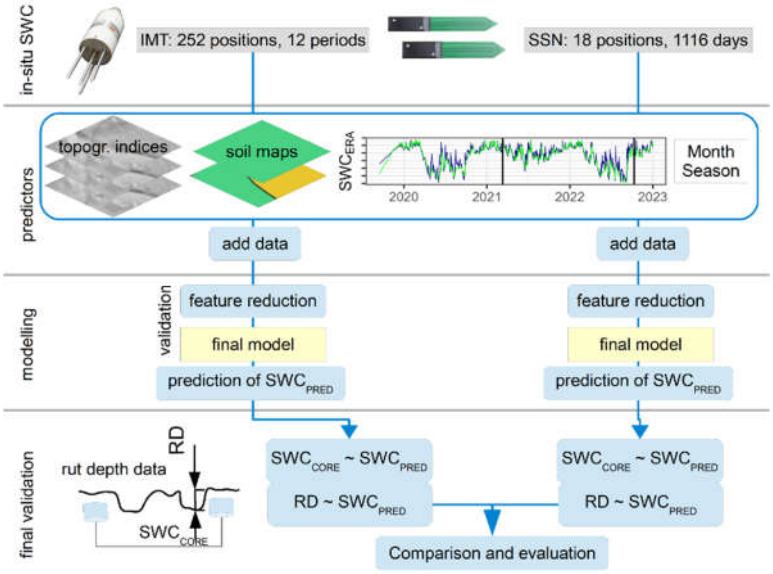

Figure 1: Soil water content (SWC, [%]) was predicted using models trained on two datasets: in-situ measurements (IMT) and soil sensor networks (SSN). Input variables included topographic indices, soil type data, SWC estimates from ERA5-Land (SWC_{ERA}), and date values. Through cross-validation, we selected the final models, used to predict SWC_{PRED} for various positions and dates during trials with a forwarder. Model estimates were compared with in-situ SWC_{CORE} and rut depth (RD, [cm]).

2.1 Study sites

The data acquisition of volumetric SWC [%] and the trials with a forwarder were conducted in two forest stands located near the city of Arnsberg in North Rhine-Westphalia (Figure 2). The forest stands were situated at an altitude of approximately 250 m on common soil types such as Cambisol and Stagnosol on Claystone and Sandstone from Devon and Carbon (Table 1).

Table 1. Characteristics of the study sites, where soil water content was captured and field trials with a forwarder were performed.

Site	**Coordinates in WGS84**		**Dominant soil types**	**Humus form**	**Slope**	**Canopy**
	x	y			[%]	
A	8.039	51.406	Cambisol - Stagnosol	Mesomull	15-30	*Fagus sylvatica, Quercus spp., Pinus sylvestris*
B	8.024	51.473	Stagnosol	Mull	1-7	*Fagus sylvatica*

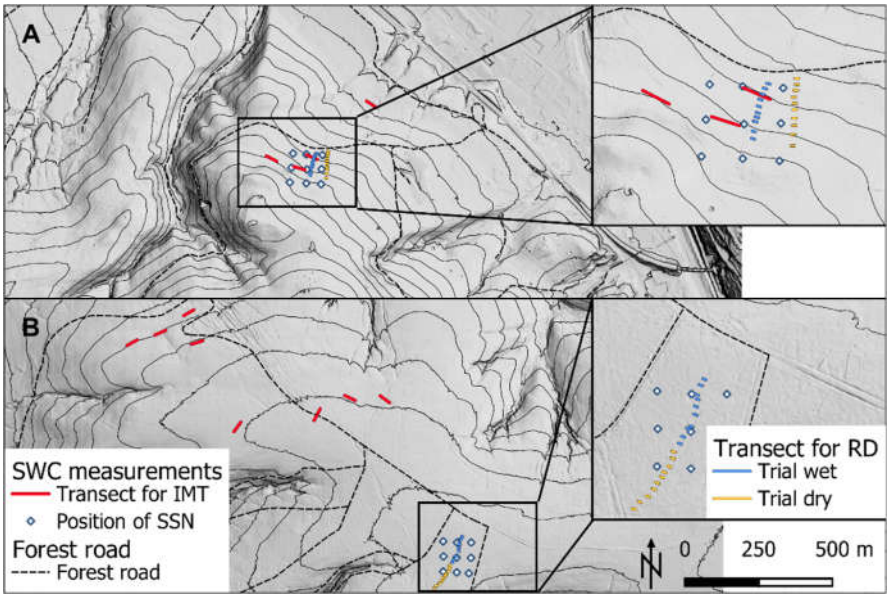

Figure 2: The map indicates the locations of two experimental areas on a hill-shaded digital elevation model with 10 m contour lines; Site A (A, coordinates x, y in WGS84: 8.039, 51.406) and Site B (B, coordinates: 8.024, 51.473), which were used for collecting time-series data on soil water content (SWC). SWC was measured using a handheld soil moisture meter (impedance measuring technique, IMT) along transects (red lines), each containing 21 measuring positions (2 m spacing). In addition, a soil sensor network (SSN) was used to continuously capture SWC at 18 positions (white rhombus). The map also indicates the locations of 40 transects (in crop-outs) used for measuring rut depth (RD) during relatively wet conditions ($Trial_{WET}$, blue lines) and dryer conditions ($Trial_{DRY}$, orange lines).

2.2 Soil moisture models

2.2.1 In-situ soil moisture

Two sets of in-situ data of soil moisture were used: 1. Manual measurements of SWC were performed using a HH2 Moisture Meter (Delta-T Devices Ltd, England), which applies Impedance Measuring Technique (i.e. 'IMT') (Eijkelkamp Agrisearch Equipment, 2013). 2. Data from a continuously measuring Soil Sensor Network (i.e. 'SSN').

The IMT data used for this study were previously used for the validation by Schönauer et al. (2022) and consisted of 12 measuring transects. The transects were placed in various positions in broadleaved forests, known to be temporarily wet or sensitive for machine traffic, with each transect having a length of 40 m. SWC was measured with a spacing of 2 m along the transects. To measure SWC, measuring rods of 60 mm length were vertically inserted into the soil after removing the humus layer. The measurements were taken almost monthly between September 2019 and October 2020 (Figure 3B). The IMT data consisted of 2,184 observations. Overall, this dataset offers a relatively high level of spatial granularity, with 252 measuring positions. However, the temporal resolution of the data is relatively low, with only monthly measuring campaigns conducted.

The SSN was launched in Dezember 2019 and its data was obtained from continuously measuring SMT100 sensors (TRUEBNER GmbH, Germany), placed on two sites, each having 9 positions with a spacing of 50x50 m. At each position, two sensors were placed at a depth of 10 cm in the mineral soil, with a temporal resolution of 15 minutes. The data from these sensors were averaged for each position and each of the 1,116 days captured (data until 2022-12-31 was included), resulting in a total of 16,351 observations after omitting all missing values. While this data set provides a high level of temporal granularity, it suffers from a low level of spatial granularity due to the limited number of positions sampled.

To enable the incorporation of seasonal effects in the modelling approaches, we transformed the date of each measurement

into numeric vectors, resulting in the variables Month and Season. The coding used for Season was as follows: 1 for March, April, and May; 2 for June, July, and August; 3 for September, October, and November; and 4 for December, January, and February.

To enable the creation of spatiotemporal data, the positions of all measuring locations were captured using post-processed signals from a GNSS device (Trimble R2 RTK Rover, Trimble, Colorado, USA). This data was then fused with a range of topographic indices. To achieve this, values of several topographic indices were extracted at each measuring position of IMT and SSN.

2.2.2 Topographic indices

For calculating topographic indices, we used a freely available digital elevation model (DEM), as provided by the Bezirksregierung Köln (2020). The resolution of this model was 1x1 m, with a vertical accuracy of ± 0.2 m. Using the free programming language R (version 4.0.2, R Core Team, 2023) and RStudio (version 2022.07.2, Posit PBC, Massachusetts, USA), along with the package "rgrass" (Bivand, 2021) to utilize GRASS GIS (Awaida and Westervelt, 2020) commands in the R interface, the command 'r.hydrodem' was used to ‘remove all sinks’ (Flags: -a) from the DEM. Thereafter, we calculated depth-to-water (DTW) maps. To generate these maps, we followed the script by Schönauer and Maack (2021) and used flow initiation areas (FIA) of the following sizes 0.25 ha (DTW025), 1.00 ha (DTW1), and 4.00 ha (DTW4), which account for different overall soil moisture conditions. A smaller FIA results in a DTW map for wetter conditions, as the network of simulated flow lines expands, while a larger FIA represents drier conditions. For further details, refer to Murphy et al. (2009; 2011).

The Topographic Wetness Index (TWI) represents the tendency for water to accumulate at any point in the catchment (Quinn et al., 1991), while the stream power index (SPI) represents the power of water flow at any point in the catchment and the gravitational forces that move water downslope (Moore et al., 1991). To compute TWI, we used the 'r.watershed' command in GRASS GIS, as conceived by Sørensen and Seibert (2007). TWI was calculated as $\ln(\alpha/\tan(\beta))$, where α is the cumulative upslope area draining through a point per unit contour length, and $\tan(\beta)$ is the local slope angle. SPI was calculated as $\alpha * \tan(\beta)$ (Moore et al., 1991). Flow Accumulation, representing the absolute amount of overland flow passing through each cell was also included as a variable. TWI, SPI, and Flow Accumulation were calculated on an aggregated DEM with a spatial resolution of 15x15 m. This resolution has been shown to exhibit a stronger correlation with SWC, and can be assumed to be more robust (Ågren et al., 2014), as observed in prior work where resolutions ranging from 1 to 20 m were tested (data not shown). In addition, we calculated the variable Slope [°] using the R-package 'raster' (Hijmans, 2020).

2.2.3 Soil maps

Soil maps of North Rhine-Westphalia were originally generated at a scale of 1:5,000 from forest site surveys. We included soil type information (Soil05) for the analysis. While these maps are not available across the entire region of North Rhine-Westphalia, they were provided for the study sites by the Geological Survey of North Rhine-Westphalia. By contrast, soil maps with a scale of 1:50,000 are available for the entirety of North Rhine-Westphalia (Soil50).

2.2.4 Temporal soil water content from ERA5-Land

ERA5-Land is a global reanalysis dataset providing hourly estimates of meteorological variables at a spatial resolution of 9x9

km, including soil moisture [$m^3\ m^{-3}$] at the top soil layer (0-7 cm, 'layer 1' (L1)) and at a depth of 7-28 cm ('layer 2' (L2)). ERA5-Land data is retrieved by assimilating satellite and atmospheric forcing (Muñoz-Sabater et al., 2021). It provides a reliable representation of soil moisture values and variations across the majority of global regions, making it applicable for various geophysical applications (Lal et al., 2022).

We utilized the API provided by CDS (Copernicus Climate Change Service, 2019) and the R-package 'ecmwfr' (Koen Hufkens et al., 2019) to download daily grids (at 14:00 UTC) of layer 1 and 2. The downloaded data covered both the whole time span of our data and the two measuring sites. Both sites were situated in one 9x9 km raster cell of the ERA5-Land. The land cover for this cell was derived from Bezirksregierung Köln (2023), showing that open land (e.g. grassland, crops) dominated with 52% of the total cover, whereas forests occurred on approximately 31% of the cell size, followed by 12% coverage from infrastructure, 3% loose material, and 2% water bodies.

After downloading the data, we stacked the daily grids and extracted the corresponding values at each measuring position, giving $SWC_{ERA}L1$ and $SWC_{ERA}L2$.

All data, the topographic information, soil types, numerical values of date and the dynamic variables from ERA5-Land were merged with in-situ data, either IMT or SSN.

2.2.5 Modelling

The modelling approach described here was applied separately for both data sets, IMT and SSN (the main outputs when both datasets were combined can be seen in Appendix A).

Initially, we fitted a linear model with SWC as the dependent variable and $SWC_{ERA}L1$, $SWC_{ERA}L2$, Month, Season, DTW025, DTW1, DTW2, DTW4, Slope, TWI, SPI, Accumulation, Soil05, and Soil50 as the independent variables. We then used this linear model to check the data for autocorrelations and subsequently eliminated variables with a variance inflation factor > 10 through an iterative process, reducing one variable at a time. Also, the feature selection according to the Boruta algorithm (package 'Boruta', Kursa and Rudnicki, 2010) was applied.

We then trained random forest models (Breiman, 2001), repeatedly reported as efficient in predicting complex data (Kemppinen et al., 2018; Carranza et al., 2021; Cavalli et al., 2023), using the 'ranger' package (Wright and Ziegler, 2017) with a 10-fold cross-validation with 5 repetitions. For each of the 50 models in the validation of one configuration, we noted the mean of Kendall's coefficient of correlation τ (since different sample sizes occurred) of the random forests and the representative standard deviation. In addition, the least important variable according to impurity and its frequency within the 50 validation sets were traced. The variable noted most frequently as least important was then removed, and a new cross-validation was performed on SWC ~ (n-1) variables, with n being the number of predictors in the model trained previously. This process was repeated until only one predictor variable remained.

To avoid temporal autocorrelations at the measuring positions, positions IDs were used to select the folds of the cross validations.

2.2.6 Selection of the final model

To select the final random forest model for each data partition, we examined the maximum τ values obtained and multiplied them by 0.99 (according to Hauglin et al. (2021)). This was done to penalize the use of an unnecessarily high number of predictor variables. We selected the model with the least number of predictor variables within this 1%-range as the final

model. The final models (built on IMT and SSN data) were then used to predict rasters of SWC_{PRED}, which were visually evaluated. Subsequently, the outputs of the final models were compared to rut depths and SWC at the machine operating trails.

2.3 Data from field trials with a forwarder

2.3.1 Rut depth (RD)

During the field trials conducted in two forest stands at two seasons, a fully loaded forwarder (John Deere 1210G, 8-Wheel model, total mass of 28 Mg (18 Mg machine weight + 10 Mg loading)) was used. The first trial was conducted on section 1 of an existing machine operating trail on 2021-03-11, during generally wet conditions ($Trial_{WET}$). The second trial was conducted on subsequent section 2 of the same machine trail on 2022-10-11, during dryer conditions ($Trial_{DRY}$) (Figure 2, Site A), or in close proximity of section 1 (Site B), as there the machine trail was not long enough for both sections.

The four trials were positioned near the sensors of the SSN (Figure 2) and, in the case of Site A, near the IMT measuring transects. On Site B, the IMT transects were at a distance of 530 m to 1300 m. Moreover, there is a temporal lag between the IMT measuring campaigns and the field trials (Figure 3). This discrepancy stems from the IMT data being collected as part of a separate research project.

The 8-wheel machine trafficked section 1 and 2 of both operating trails, and made four passes. Before the first machine pass, the initial surface was captured along 10 perpendicular transects on each of the four sections. These 4 m wide transects were placed and marked permanently with inserted wooden pegs. The same pegs were used to position the beam, which served as the reference height to measure profiles along each transect. Into this beam, metric scales were inserted with a spacing of 10 cm in between, to note the distance between the surface and the beam to the nearest cm. These measured distances (D0, [cm]) describe the surface along the transect on already existing machine operating trails, prior to the trial conducted in this study. The same procedure was repeated after the fourth consecutive machine passes, giving D4 [cm].

Next, the differences between D0 and D4 were calculated at each of the 41 measurements (10 cm spacing over 4 m) along a transect. The maximum value of these differences, measured at the left or right machine track, was used to determine rut depth (RD, [cm]). We used average values of both tracks to prevent pseudo replicates, since intraclass correlation coefficient was high (0.83), when left and right tracks were integrated separately. Moreover, mean and maximum values of rut depth were highly correlated (adj. $R^2 = 0.96$).

2.3.2 Soil water content at the rut depth transects (SWC_{CORE})

Volumetric soil moisture content was captured outside the 1st, 4th, 7th and 10th transect of each section, with a distance of 1 m to the left and right track, at a depth of 10-15 cm. This water content was determined using 100 cm³ cores taken with an undisturbed core sampler, with three replicates at each measurement. SWC_{CORE} was calculated according to equation (1):

$$SWC_{CORE}[\%] = \frac{M2 - M1}{M1} * 100 \quad (1),$$

with M2 being the fresh mass of the soil taken with undisturbed cores and M1 being the mass after drying the samples in oven with 105 °C, until mass constancy was reached.

Measurements of RD and SWC_{CORE} were georeferenced using the GNSS devise and complemented with all the predictor variables, as described above.

2.4 Comparisons between model predictions and RD or SWC_{CORE}

For the 'testing on rut depth data' (Figure 1), values of SWC_{PRED} were compared to RD or soil water content, captured through undisturbed cores along the transects, SWC_{CORE}. Therefore, the predictor variables from the rut depth dataset were used to predict SWC_{PRED} by means of the final random forest models created in the soil moisture modelling. Since the goodness-of-fit between in-situ values of RD or SWC_{CORE} and SWC_{PRED} was to some degree sensitive to the seed set during modelling, we repeated the predictions ten times and used average values to receive robust estimates of SWC_{PRED}. To test the correlations between paired samples of SWC_{CORE} or RD and SWC_{PRED}, Kendall's rank correlation was used. We illustrated the corresponding p-values as follows: `***` for p<0.001, `**` for 0.001-0.01, `*` for 0.01-0.05, (`*`) for 0.05-0.10 and 'ns' for p-values being higher than 0.10. Values are given as mean±standard deviation.

3 Results

3.1 Soil water content

The mean value of SWC, measured using a handheld moisture meter (IMT), varied between 13.0±10.0% in August 2020 and 43.2±5.95% in February 2020 (Figure 3). Daily mean values obtained from soil sensor networks (SSN) were similar to those obtained from IMT, ranging from 13.8±2.90% in September 2020 to 39.1±6.66% in March 2020, in the period that corresponds to the one covered by IMT. The driest conditions were observed in September 2022, with a daily mean SWC of 12.7±2.55%. Overall, the results suggest that IMT and SSN provide comparable estimates of SWC, with the latter providing higher temporal resolution at a low spatial granularity.

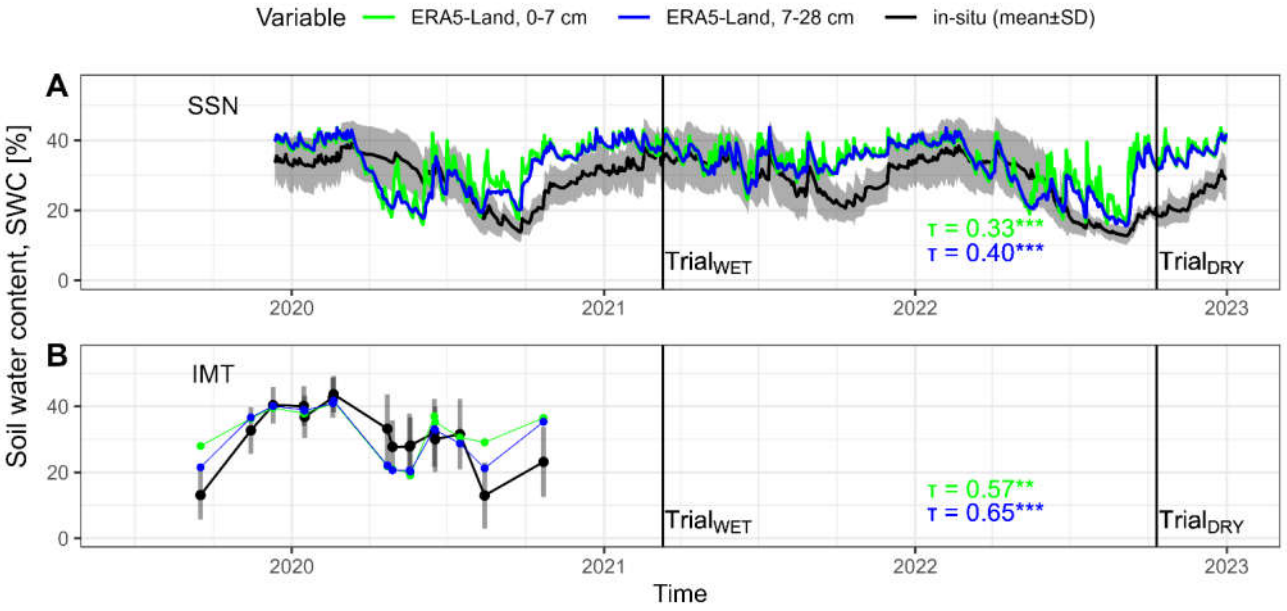

Figure 3: Time series of soil water content (SWC) measured using a soil sensor network SSN (A) with 18 measuring positions on two sites and manual measurements, using impedance measuring technique IMT (B) conducted on 252 positions (black lines/points show daily mean values, grey shading/bars show standard deviation for each day). SWC retrievals from ERA5-Land are shown as a blue line/point (0-7 cm vertical resolution, as available from Copernicus Climate Change Service (2019)) and a green line/point (7-28 cm vertical resolution). The goodness-of-fit between daily means of measured SWC and ERA5-Land retrievals is reported

using Kendall's rank correlation coefficient (τ). Vertical lines indicate the dates of the trials when a forwarder conducted four passes at existing machine operating trials.

3.2 Soil moisture models

The positions IDs were used to select the 10 folds for cross-validation. However, the dataset SSN had only 18 measuring positions (where SWC was measured on 1116 days), resulting in relatively high deviations of Kendall's τ of the random forests. The most important feature for this dataset was given by DTW025, although the resulting quality was low, with τ of 0.363±0.198. By adding the temporal component Month, the τ improved to 0.637±0.065, which had the lowest standard deviation for the repeated folds. The final model for this dataset included the temporal variables Month and $SWC_{ERA}L2$, as well as the topographic predictor variables TWI and DTW025 (Figure 4). The resulting τ was 0.710±0.095, revealed through the cross-validation.

For the IMT partition, which had a low temporal but high spatial resolution, the most important feature was the temporal information $SWC_{ERA}L2$, leading to a τ of 0.569±0.036. The final model had an τ of 0.620±0.016, including the predictor variables $SWC_{ERA}L2$, Month, Season, and DTW025, TWI, SPI and DTW4.

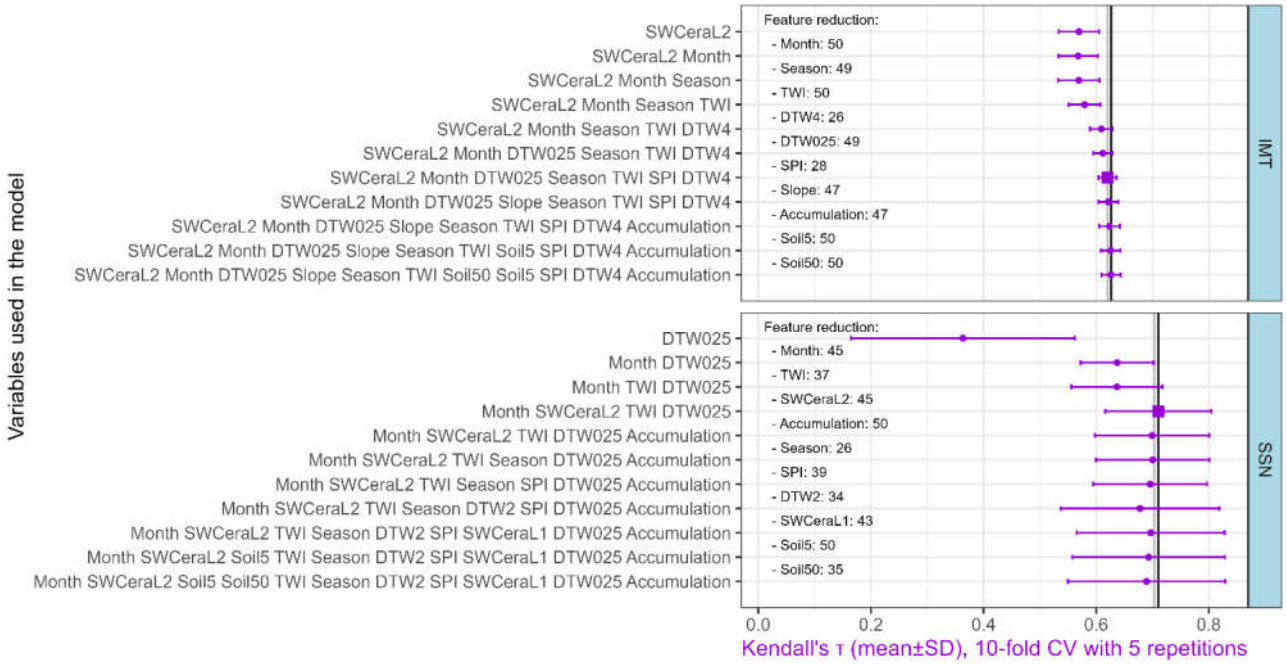

Figure 4: Soil water content (SWC) was modelled by random forests (RF), and evaluated by a repeated 10-fold cross validation (CV). Mean values and standard deviation of resulting values of the Kendall rank correlation coefficient τ during the CV are shown. A stepwise elimination of the least important variable was performed, and the frequency of this variable over all models is provided ("Feature reduction"). The vertical lines indicate the maximum value of τ (black) and the 99% of the maximum (grey), to select final models (squares). Variables used are described in section 2.

3.2.1 Comparisons of SWC_{CORE} with SWC_{PRED}

The final random forest models of both, the IMT and SSN dataset, were used to calculate SWC_{PRED} on the predictor variables of the rut depth data, including SWC_{CORE} measured at the outside of a subsample of the measuring tracks by undisturbed cores. The comparison between SWC_{CORE} and SWC_{PRED} values predicted by the final random forest models of both datasets (SSN and IMT), revealed a significant association (Figure 5).

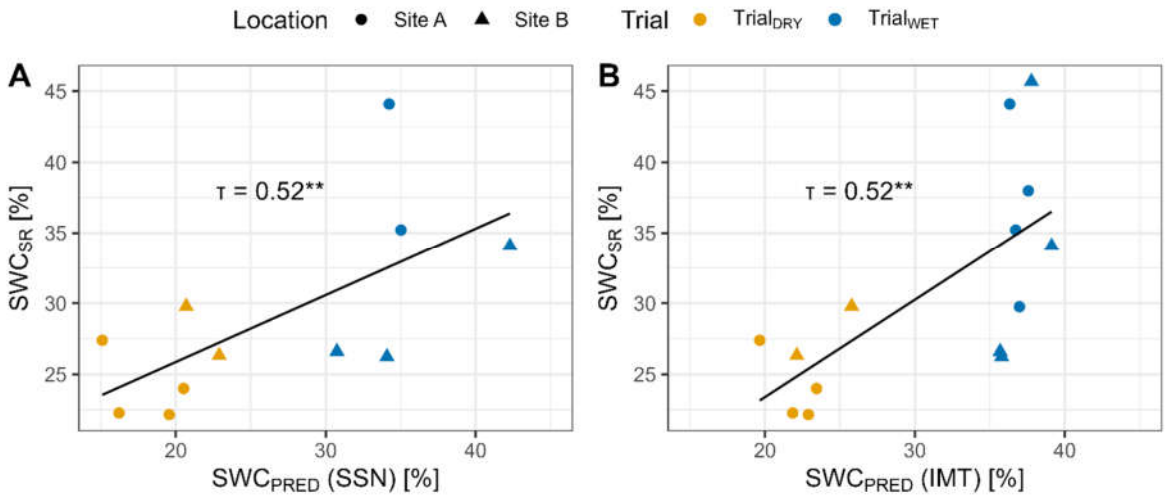

Figure 5: Soil water content was measured during two trials with a forwarder along a machine operating trail (n=14), using 100 cm³ undisturbed cores (SWC_{CORE}), and compared to values predicted (SWC_{PRED}) by a model trained data from a continuously measuring soil sensor network (SSN, A), or manual measurements with a handheld moisture meter (IMT, B). Correlations were evaluated using Kendall's τ and significance levels are indicated by * * * for p<0.001, * * for 0.001-0.01, * for 0.01-0.05, (*) for 0.05-0.10, and 'ns' for p>0.10.

3.3 Interrelations between rut depth and topographic indices or SWC

Rut depth (RD, [cm]) was measured during four trials with a forwarder, covering 10 transects for each trial. This provided us with the potential for 40 measurements, but unfortunately, 4 of them were not ascertainable as the forwarder destroyed the wooden pegs that positioned the reference beam. In $Trial_{WET}$, conducted in March 2021, $SWC_{ERA}L1$ and $SWC_{ERA}L2$ showed a soil moisture level of 39%. At Site A, the measured RD was 10.3±1.9 cm, while at Site B, the RD was 12.7±5.5 cm, with the highest value of RD recorded after 4 passes, with a depth of 21.5 cm. In $Trial_{DRY}$, conducted in October 2022, the soil water content from ERA5-Land was 32%. At Site A, the measured RD was 3.5±1.7 cm, and at Site B, the RD was 4.3±1.2 cm.

3.3.1 Comparisons of RD with DTW and TWI

Considering the significance of the topographic indices DTW and TWI in the development of the SWC models (Figure 4), we aimed to compare RD with both indices. Notably, RD exhibited a clear correlation with DTW025, the most conservative DTW scenario (Figure 6). TWI also demonstrated a correlation with RD.

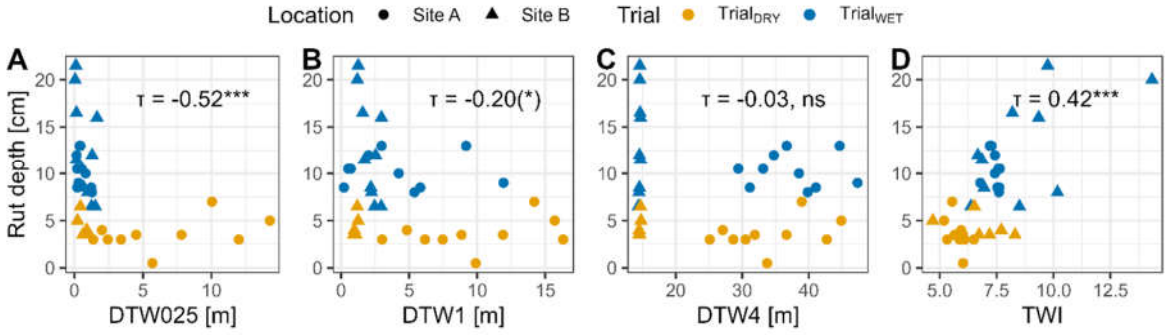

Figure 6. Rut depth (RD) was determined after four passes of a forwarder, driving on two Sites (A and B), during two conditions

($Trial_{WET}$ and $Trial_{DRY}$). RD was compared to the topographic indices depth-to-water (DTW), calculated with different flow initiation areas (0.25 – 4.00 ha), and the topographic wetness index. Correlations were evaluated using Kendall's τ and significance levels are indicated by * * * for p<0.001, * * for 0.001-0.01, * for 0.01-0.05, (*) for 0.05-0.10, and 'ns' for p>0.10.

While showing significant correlations, the nature of these static maps does not allow for the representation of current moisture conditions. This limitation was overcome when using the predicted (or observed) values of SWC.

3.3.2 Comparisons of RD with SWC_{CORE} and SWC_{PRED}

RD was positively correlated with SWC_{CORE} when both trials with different moisture conditions were included in testing (Figure 7A). However, when each trial was tested separately, no correlation between RD and SWC_{CORE} was observed. Compared to the correlation between RD and SWC_{CORE}, modelling outputs SWC_{PRED} proved to be a better predictor of rut depth, particularly for $Trial_{WET}$. The final models that were selected for both datasets produced a Kendall's τ of 0.61 (for IMT, Figure 7B, and SSN, Figure 7C), when comparing RD of the four trials with the corresponding SWC_{PRED}. Although the R^2 values for these models were in similar range (0.620 fot IMT and 0.549 for SSN), we chose to use Kendall's τ since different sample sizes were involved in the analysis. This was particularly relevant for comparing RD with SWC_{PRED} for each Trial separately. While no correlation could be found for $Trial_{DRY}$, correlations were found for $Trial_{WET}$, with Kendall's τ of 0.344 (p=0.037) and 0.281 (p=0.090), for the final models trained on IMT and SSN, respectively (Figure 7B,C). Yet, these correlations seem to fragile, as a difference of a few percent of predicted SWC_{PRED} (IMT) is associated with the range of RD between 6.5 and 21.5 cm. Moreover, when analysing the sites separately, a vage trend between SWC_{PRED} and RD could be observed, but without showing significant correlations (Appendix B).

Since the final model trained on IMT data performed slightly better in $Trial_{WET}$ compared to the model trained on SSN data (Figure 7), we chose the IMT model for the generation of prediction rasters for the days of interest (Figure 7B1,B2).

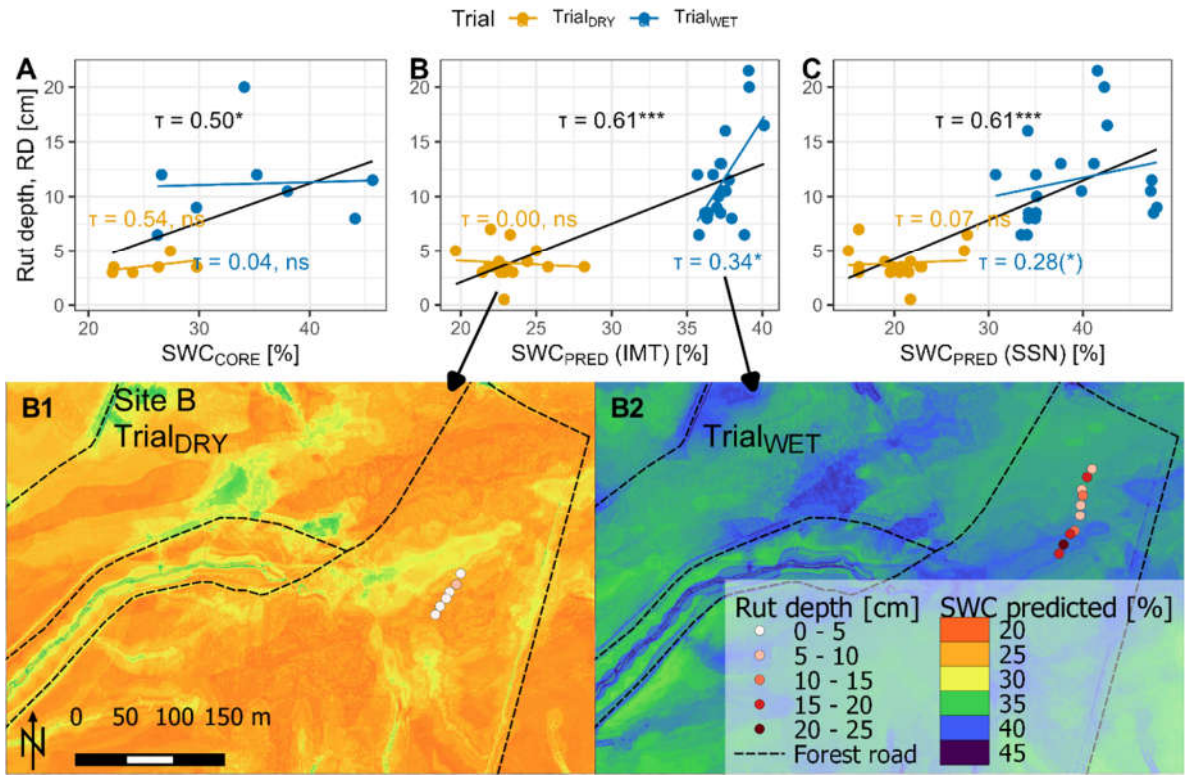

Figure 7: Rut depth (RD) was determined after four passes of a forwarder, driving on two Sites, during two conditions (WET and DRY). RD was compared to SWC values, determined for undisturbed soil cores (A) and SWC values predicted by a random forest model trained on manually obtained IMT measurements (B, see Figure 1) and predicted by a model trained data from a continuously measuring soil sensor network (SSN, C). Correlations were evaluated using Kendall's τ. The correlation of all values is given in black, blue and yellow show the Trials during wet and dry conditions.Significance levels are indicated by * * * for p<0.001, * * for 0.001-0.01, * for 0.01-0.05, (*) for 0.05-0.10, and 'ns' for p>0.10. The model based on IMT data (B) was used to calculate prediction rasters for the days of the field trials (B1, B2).

4 Discussion

4.1 Importance of predictive systems

Wet soils are prone to soil disturbances like the formation of deep ruts (McNabb et al., 2001; Poltorak et al., 2018), since water implies a reduction of particle-to-particl bondings within the soil (Hillel, 1998), decreasing the restistance to external forces. Consequently, accurate predictions of soil water content (SWC) and soil trafficability is essential for sustainable forest management and cost-effective, environmentally friendly harvesting operations (Murphy et al., 2007; Vega-Nieva et al., 2009; White et al., 2012; Mohtashami et al., 2017; Mattila and Tokola, 2019; Picchio et al., 2020; Uusitalo et al., 2020). Topographic modelling requires minimal input and the temporal variables used in the final model presented here, are freely available (Copernicus Climate Change Service, 2019). A spatiotemporal model predicting SWC could improve the guidance of machine operators in forest sites during harvesting operations, for example by the effective positioning of brush mats (Labelle and Jaeger, 2018; Labelle et al., 2019). Practical use of static, topographic maps has already been observed in Canada and Scandinavian countries (Ring et al., 2022). By incorporating a temporal aspect, the accuracy of these tools could be further improved. This has the potential to enhance sustainable forest management by protecting soil and mitigating harmful sediment

transport (White et al., 2012; Ågren et al., 2015; Kuglerová et al., 2017; Lidberg et al., 2020).

4.2 Comparison to previous work on predictions of SWC

Since soil moisture predictions are crucial for a variety of forestry aspects, several publications have focused on this topic before. For example, Lidberg et al. (2020) predicted soil moisture classes using spatial models built on topographic indices, correctly classifying 73% of wet areas in a Swedish case study. Ågren et al. (2014) reported accurate predictions for 87-92% of observations by comparing soil moisture classes to DTW maps. Larson et al. (2022) used data from the Krycklan catchment and found an accuracy of 84% when comparing moisture classes to the recently developed 'SLU soil moisture map' (Ågren et al., 2021). However, these validations were based on static topographic maps. One attempt to make such static maps dynamic was realized within the DTW concept, which can be customized to calculate various scenarios to adjust to general moisture conditions (e.g., flow initiation areas of 0.25, 1, and 4 ha for wet, moist, and dry conditions, respectively), but selecting the most appropriate scenario during practical use can be a challenging task that requires significant expertise (White et al., 2012; Leach et al., 2017; Lidberg et al., 2020). To overcome this challenge, we aimed for improvement of soil moisture prediction and refined the spatiotemporal approach conceived by Schönauer et al. (2022). During cross-validation of IMT data from sites in Finland, Poland, and parts of the data used in this work, they reported an R^2 of 0.80. The models for the present study showed an R^2 of 0.759±0.136 (SSN) or 0.636±0.040 (IMT), corresponding to Kendall's τ of 0.710±0.095 or 0.620±0.016, respectively. Although this may not seem like an improvement, it should be noted that the data from German sites had less explanatory power of topography for predicting SWC. For example, DTW4 alone explained SWC to a very limited extent ($R^2 = 0.037$***).

4.3 Prediction of rutting

Besides the comparisons of SWC with DTW maps, various studies have also investigated the capability of topographic indices in predicting rutting – with conflicting outcomes. For example, Vega-Nieva et al. (2009) found that 65% of ruts deeper than 25 cm were located in areas with a DTW value of less than 1 m, and 93% of these ruts occurred in areas with DTW values less than 10 m. Similarly, Heppelmann et al. (2022) observed a high frequency of severe rut depth in areas with DTW values less than 1 m in Norway. However, Mohtashami et al. (2017) did not find evidence of such patterns in a field trial where the inclusion of DTW values did not improve the accuracy of a linear model to describe the extents and degrees of rut depth on machine operating trails. In agreement, Schönauer et al. (2021a) found no evidence that DTW or TWI could predict rut depth in a field trial conducted in a temperate broadleaved stand. In this study, we found a significant correlation between RD and DTW025 with a Kendall's correlation coefficient (τ) of -0.52***. Yet, this correlation has to be seen with caution: It is mainly driven by differing ranges of RD between the two Trials, as can be seen in Figure 6A. We observed that the temporal adjustments of the model based on current moisture conditions improved predictions of rutting by up-to-date SWC predictions, leading to a τ of 0.61*** (Figure 7B,C). While a strong association between RD and predicted values of SWC was observed, the influence of differences between the trials is evident. However, the ranges of RD for each trial were consistent with the SWC predictions. In $Trial_{WET}$, a significant correlation between RD and SWC_{PRED} was observed (Figure 7B). We hypothesize that the wetter conditions during this trial, which lead to soil destabilization (Hillel, 1998; McNabb et al., 2001), enhanced the predictive power of topographic indices representing soil water distributions. For instance, DTW025 overlapped with surface water in depressions, as observed in the field campaigns for $Trial_{WET}$.

In contrast, during $Trial_{DRY}$, no correlation was found between RD and SWC_{PRED}. SWC along the measuring sections was likely below the threshold for soils to become susceptible to deformation. For example, Poltorak et al. (2018) stated that ruts only occurred on soils with an SWC above 50%, whereas SWC_{CORE} at $Trial_{DRY}$ was below 30% (Figure 5).

4.4 Description of the model

The best-performing model in predicting RD incorporated temporal information from $SWC_{ERA}L2$, Month and Season, as well as spatial information from DTW025, TWI, SPI and DTW4, and was based on data from the manual measurements (IMT). The IMT data was collected in close proximity to the rut depth measurements at Site A (Figure 2), or with a distance of up to 1.3 km at Site B. However, the spatial distance between the IMT training data and the rut depth data did not seem to be crucial for the accuracy of predicting rut depth (Appendix B), since Kendall's τ between RD and SWC_{PRED} was similar for both sites. Surprisingly, the correlation between in-situ SWC_{CORE}, sampled directly at the machine operating trails, showed a lower explanatory power in predicting RD than SWC_{PRED}. Although an overall association between RD and SWC_{CORE} was confirmed, no correlation could be found when trials were analysed individually.

4.4.1 Temporal variaton was higher than spatial variation

This indicates that the temporal variability in soil moisture between the trials was more important in this study than the spatial variability within the relatively small areas where each trial was conducted. The spatial distrubition of the rut depth measurements might have been limiting in the present work. The semivariogram indicates the spatial covariation of rut depth and SWC (Figure 8). While the covariation of RD in Sita A is indicated to be high within a range of 10 m (RD-transects were at this distance), on Site B during wet conditions, the sill of the semivariogram reaches almost 40 m, which covered a high number of transects. Similarly, excluding soil information in the initial stages of feature reduction suggests homogeneous soil properties on the relatively small study area.

Therefore, we have to admit, that the study design was not ideal for assessing the ability to predict rutting with a spatiotemporal model of SWC, and the results have to be considered with caution.

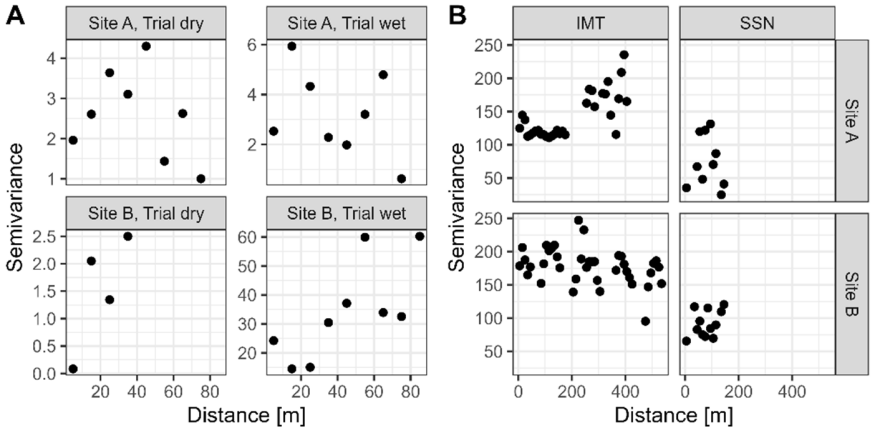

Figure 8. Semivariogram illustrating spatial autocorrelation of (A) rut depth (cm) and (B) soil water content (SWC) across the study area. Rut depth was measured during two moisture conditions, at four machine operating trail sections, allocated on two sites. The measuring transects had a spacing of 10 m. SWC was measured with handeld measuring techniques (IMT), or a soil sensor network (SSN) (Figure 2).

The spatiotemporal model (IMT), also supports the conclusion that spatial variations were wether underrepresented by the

study design (or very low compared to temporal variation by nature) as the temporal feature $SWC_{ERA}L2$ was selected as most important variable and the difference between the model with one predictor variable vs. the final model was small (Figure 4). Still, this slight increase in the models' quality allowed for the integration of spatial patterns and resulted in the significant but vague prediction of RD in $Trial_{WET}$ ($\tau = 0.344$*, Figure 7). Another indication of the integration of spatial patterns can be interpreted by the segregation of the temporal range of the IMT data (2019-2020) and the actual Trials (March 2021 and October 2022, Figure 3), indicating a generalization of spatial and temporal patterns.

4.4.2 Most important variables

In the final model (IMT), $SWC_{ERA}L2$ has been identified as the most important variable, followed by Month and Season. It is noteworthy that in the data with broader spatial coverage (i.e. IMT), in contrast to the SSN data, dynamic variables took precedence over predictor variables. Surprisingly, when modelling SSN data, characterized by high temporal resolution and low spatial resolution, DTW025 remained the most influential variable. One might have anticipated the opposite, expecting a topographic index to play a central role in modelling IMT data, and dynamic SWC_{ERA} variables dominating the modelling of SSN data.

We presume that the low spatial variations of SWC in comparison to temporal variations, inadequately represented by the provided topographic information, may have contributed to this unexpected outcome. Furthermore, the wider spatial coverage in the IMT data likely resulted in more robust averages of SWC, leading to a stronger correlation with the coarse spatial data of ERA5-Land (9x9 km). On the contrary, the SSN data, originating from areas with a size of 100x100 m and known for their temporal wetness, could explain the heightened importance of DTW025. Some sensors might have measured constant water saturation, thereby inflating the explanatory power of topographic information. These assumptions are speculative, and further research in this direction is warranted.

In the feature reductions of IMT and SSN data (Figure 4), $SWC_{ERA}L2$ (7-28 cm soil depth) dominated over $SWC_{ERA}L1$ (0-7 cm). This aligns with in-situ measurements of SWC by the SSN, conducted at a soil depth of approximately 10 cm (Figure 3A). Even for the IMT data, where SWC was measured in the top 6 cm of soil, $SWC_{ERA}L2$ yielded a better goodness-of-fit compared to $SWC_{ERA}L1$ (Figure 3B). We hypothesize that the prevalence of open lands as the dominant land cover form in the ERA5-Land raster cell (section 2.2.4) contributed to the superior fit of $SWC_{ERA}L2$. Grasslands typically exhibit higher temporal heterogeneity of soil moisture compared to forests (James et al., 2003). This temporal heterogeneity tends to decrease with deeper soil layers (Tromp-van Meerveld and McDonnell, 2006). Therefore, the stronger correlation between $SWC_{ERA}L2$ and SWC, as well as its higher importance within the random forests, seems reasonable. The disparity between SWC_{ERA} and in-situ SWC can be attributed to the high transpiration rates in forests, as opposed to grass (Kelliher et al., 1993).

4.5 Further developments

The terrain data was derived from a digital elevation model, which is increasingly available for the entire Europe (Hoffmann et al., 2022), while the dynamic variables are based on date and retrievals from ERA5-Land, which are freely available up to a few days ago. These inputs would allow for automated mapping of current soil water content, which could be made accessible to forestry stakeholders. Recent developments also show a pathway to integrate medium and long range weather forestcasts into trafficability predictions, as conceived by the Finnish Meteorological Institute (2023). Both, recent as well as forecasting predictions can lead to improved soil protection, higher efficiency of timber harvesting (Suvinen and Saarilahti,

2006), and a new stage of sustainable forest management (Campbell et al., 2013; Jones and Arp, 2019; Uusitalo et al., 2019; D'Acqui et al., 2020). However, it should be noted that the in-situ data of SWC originated from manual measurements, and it was relatively labor-intensive to gather this amount of data. There is potential to reach appropriate accuracy even with a reduced dataset - further investigation would be necessary to determine the essential input data criteria. The alternative to manual measurements is given by sensor networks, which led to comparable results, but such sensor networks are expensive to establish and maintain. Nonetheless, initiatives of installing sensors are emerging and additional manual measurements could be conducted. In the future, forestry stakeholders who require accurate raster predictions could potentially facilitate manual measurements or install sensors and provide the captured data to scientific organizations, which could deliver spatiotemporal soil moisture predictions in return. The captured data could be made available for creating spatiotemporal models of SWC, allowing for additional training data and daily raster predictions for new areas of interest, with various scientific insights and practical applications.

Conclusion

In this study, we developed a spatiotemporal model that used multiple topographic indices, temporal variables, soil moisture retrievals from ERA5-Land, and data from manual measurements to predict soil water content (SWC). Predicted values of SWC were compared to rut depth data collected during four forwarder trials. Overall, the model performed well in predicting rut depth, with a Kendall's τ of 0.61 for all trials. Yet, this result has to be considered with caution, since spatial covarition was detected in parts. We hope, that this experience helps for future research, in which more attention to spatial covariaton on soils should be paid. Still, we believe that a dynamic prediction of SWC will help forest managers and machine operators avoid wet areas, leading to more sustainable forest operations. Using freely available temporal information is a significant improvement, as it enables more accurate and up-to-date predictions, which allow to make more informed decisions and avoid potential hazards. Future work should focus on developing automated pathways for generating daily raster predictions of SWC, and on generating reliable and comprehensive in-situ data. There is a need for more data on rutting and SWC, measured with a sufficient spatial coverage, whether by manual measurements, the establishment of additional sensor networks, or by automatic ways of capturing rut depth data through machines driving off-road, to cover more areas and different sites and regions.

Data availability

The data used in this work will be made accessible via Zenodo

Author contribution

MS and DJ designed the experiments and MS and FH carried them out. MS developed the model code and performed the simulations. MS prepared the manuscript with contributions from all co-authors.

Competing interests

The authors declare that they have no conflict of interest.

Acknowledgements

We acknowledge the financial support from the Eva Mayr-Stihl Stiftung for this work. We extend our gratitude to the Geological Survey of Northrhine-Westphalia (Landesbetrieb NRW) for conducting the soil mapping on the experimental sites and for their contributions to the field trials analysis. In particular, we would like to thank Dr. Heinz Peter Schrey, Dirk Elhaus,

Thilo Simon, and Rainer Janssen. Our appreciation also goes to the Forest Education Centre, Forstliches Bildungszentrum, Zentrum für Wald und Holzwirtschaft, Landesbetrieb Wald und Holz NRW, Arnsberg, Germany, for their valuable support during the fieldwork. Special thanks to Thilo Wagner and Thomas Späthe for their efforts in organizing the field trials, and to Michael Schulte for operating the forwarder. ChatGPT (OpenAI, San Francisco, CA, USA) provided assistance in sentence editing – all content was generated solely by the authors.

Funding

This work was supported by the cooperation project "BefahrGut" funded by the State of North Rhine-Westphalia, Germany, through its Forest Education Centre, Forstliches Bildungszentrum, Zentrum für Wald und Holzwirtschaft, Landesbetrieb Wald und Holz NRW, Arnsberg, Germany; by the Bio Based Industries Joint Undertaking under the European Union's Horizon 2020 research and innovation program, TECH4EFFECT Knowledge and Technologies for Effective Wood Procurement— project, [grant number 720757].

5 Appendix

Appendix A

To model the dataset consisting of both IMT and SSN data, the procedure described in section 2 was followed. The IMT dataset was merged with a subsample of the SSN dataset, where the sample size of the SSN part was twice that of the IMT dataset. This was done to prevent over-weighting of the SSN dataset. The resulting combination of IMT and SSN data was called the "Mix" dataset.

The final model using the Mix dataset included the input variables $SWC_{ERA}L2$, Month, TWI, $SWC_{ERA}L1$, DTW025, Season, DTW1 and DTW4, and achieved a τ of 0.655±0.081 (which corresponded to R^2 values of 0.639±0.108). Supplementary Figure 1 shows that the correlation between the model outputs (SWC_{PRED}) and rut depth (RD) was significant.

Since the models trained on the Mix dataset did not perform better than those trained on the IMT or SSN datasets, we did not investigate the fused data partition any further, as one research question addressed the use of different data origins. For future work, however, the fused data would provide additional information, as compared to the individual datasets.

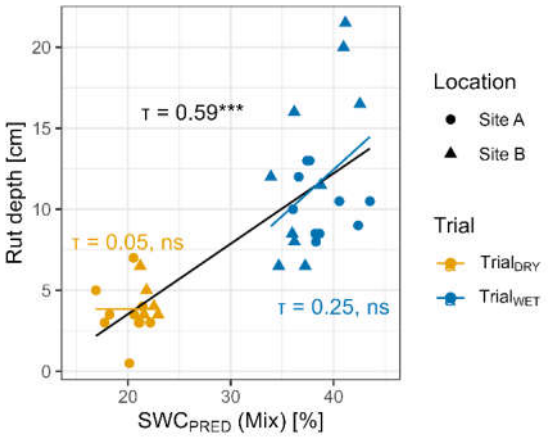

Supplementary Figure 1: Rut depth (RD) was determined after four passes of a forwarder, driving on two Sites (A and B), during two seasons ($Trial_{WET}$ and $Trial_{DRY}$). RD was compared to SWC values predicted by a random forest model trained on data from manual measurements or captured through a continuously measuring soil sensor network ('Mix'). Correlations were evaluated using Kendall's τ and significance levels are indicated by *** for p<0.001, ** for 0.001-0.01, * for 0.01-0.05, (*) for 0.05-0.10, and 'ns' for p>0.10.

473 **Appendix B**

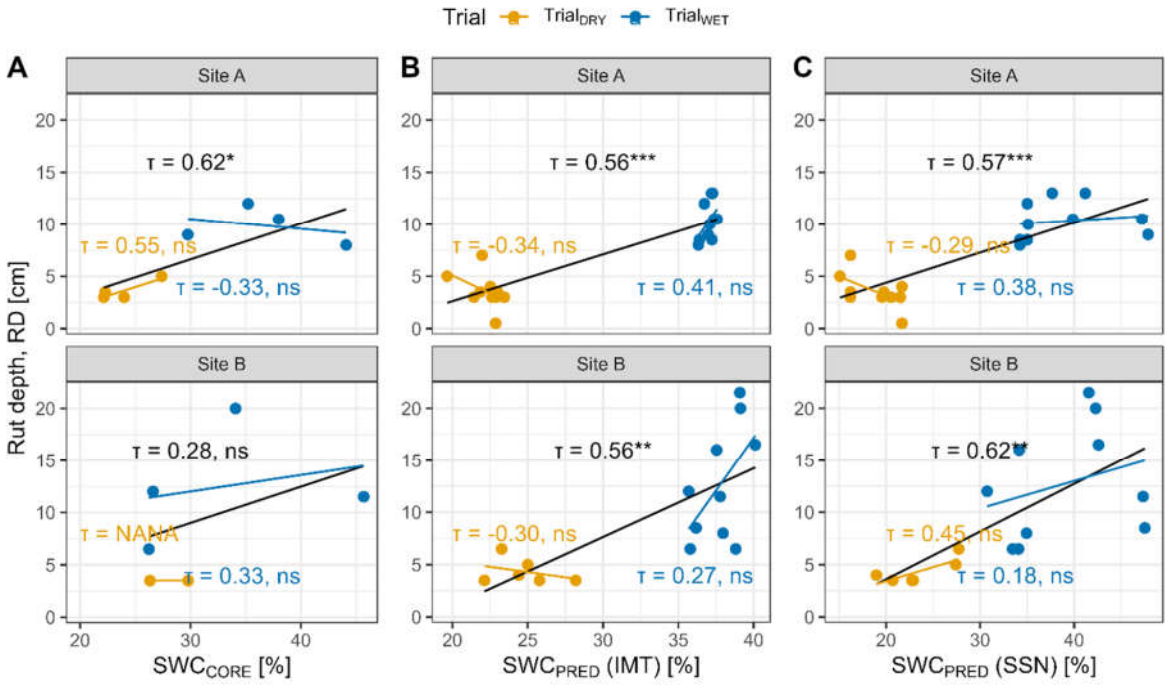

Supplementary Figure 2. Rut depth (RD) was determined after four passes of a forwarder, driving on two Sites (A and B, Figure 2), during two seasons ($Trial_{WET}$ and $Trial_{DRY}$, conducted under different moisture conditions). RD was compared to SWC values, determined for undisturbed soil cores (A) and SWC values predicted by a random forest model trained on manually obtained IMT measurements (B, see Figure 1) and predicted by a model trained data from a continuously measuring soil sensor network (SSN, C). Correlations were evaluated using Kendall's τ. The correlation of all values is given in black, blue and yellow show the Trials during wet and dry conditions.Significance levels are indicated by * * * for p<0.001, * * for 0.001-0.01, * for 0.01-0.05, (*) for 0.05-0.10, and 'ns' for p>0.10.

474

6 REFERENCES

Ågren, A., Larson, J., Paul, S. S., Laudon, H., and Lidberg, W. (2021). Use of multiple LIDAR-derived digital terrain indices and machine learning for high-resolution national-scale soil moisture mapping of the Swedish forest landscape. *Geoderma* 404, 115280. doi: 10.1016/j.geoderma.2021.115280

Ågren, A., Lidberg, W., and Ring, E. (2015). Mapping Temporal Dynamics in a Forest Stream Network—Implications for Riparian Forest Management. *Forests* 6, 2982–3001. doi: 10.3390/f6092982

Ågren, A., Lidberg, W., Strömgren, M., Ogilvie, J., and Arp, P. (2014). Evaluating digital terrain indices for soil wetness mapping – a Swedish case study. *Hydrology and Earth System Sciences* 18, 3623–3634. doi: 10.5194/hess-18-3623-2014

Ala-Ilomäki, J., Lindeman, H., Mola-Yudego, B., Prinz, R., Väätäinen, K., Talbot, B., et al. (2021). The effect of bogie track and forwarder design on rut formation in a peatland. *International Journal of Forest Engineering* 45, 1–8. doi: 10.1080/14942119.2021.1935167

Allman, M., Jankovský, M., Messingerová, V., and Allmanová, Z. (2017). Soil moisture content as a predictor of soil disturbance caused by wheeled forest harvesting machines on soils of the Western Carpathians. *Journal of Forestry Research* 28, 283–289. doi: 10.1007/s11676-016-0326-y

Ampoorter, E., van Nevel, L., Vos, B. de, Hermy, M., and Verheyen, K. (2010). Assessing the effects of initial soil characteristics, machine mass and traffic intensity on forest soil compaction. *Forest Ecology and Management* 260, 1664–1676. doi: 10.1016/j.foreco.2010.08.002

Awaida, A., and Westervelt, J. (2020). Geographic Resources Analysis Support System (GRASS GIS). USA: Geographic Resources Analysis Support System (GRASS GIS) Software, https://grass.osgeo.org

Beylich, A., Oberholzer, H.-R., Schrader, S., Höper, H., and Wilke, B.-M. (2010). Evaluation of soil compaction effects on soil biota and soil biological processes in soils. *Soil and Tillage Research* 109, 133–143. doi: 10.1016/j.still.2010.05.010

Bezirksregierung Köln (2020). *Digitales Geländemodell DGM1 [Digital elevation model]*. Accessed November 08, 2021, https://www.bezreg-koeln.nrw.de/brk_internet/geobasis/hoehenmodelle/digitale_gelaendemodelle/gelaendemodell/index.html

Bezirksregierung Köln (2023). *Landbedeckung NRW*. Accessed November 16, 2023, https://www.bezreg-koeln.nrw.de/geobasis-nrw/produkte-und-dienste/luftbild-und-satellitenbildinformationen/aktuelle-luftbild-und-3

Bivand, R. S. (2021). rgrass7: Interface Between GRASS 7 Geographical Information System and R, https://CRAN.R-project.org/package=rgrass7

Breiman, L. (2001). Random forests. *Machine Learning* 45, 5–32. doi: 10.1023/A:1010933404324

Cambi, M., Certini, G., Neri, F., and Marchi, E. (2015). The impact of heavy traffic on forest soils: A review. *Forest Ecology and Management* 338, 124–138. doi: 10.1016/j.foreco.2014.11.022

Campbell, D. M.H., White, B., and Arp, P. (2013). Modeling and mapping soil resistance to penetration and rutting using LiDAR-derived digital elevation data. *Journal of Soil and Water Conservation* 68, 460–473. doi: 10.2489/jswc.68.6.460

Carranza, C., Nolet, C., Pezij, M., and van der Ploeg, M. (2021). Root zone soil moisture estimation with Random Forest. *Journal of Hydrology* 593, 125840. doi: 10.1016/j.jhydrol.2020.125840

Cavalli, A., Francini, S., McRoberts, R. E., Falanga, V., Congedo, L., Fioravante, P. de, et al. (2023). Estimating Afforestation Area Using Landsat Time Series and Photointerpreted Datasets. *Remote Sensing* 15, 923. doi: 10.3390/rs15040923

Chen, T., He, T., Benesty, M., Khotilovich, V., Tang, Y., Cho, H., et al. (2021). *xgboost: Extreme Gradient Boosting*.

513 Accessed November 09, 2021, https://CRAN.R-project.org/package=xgboost
514 Copernicus Climate Change Service (2019). *ERA5-Land hourly data from 2001 to present*. ECMWF.
515 Crawford, L. J., Heinse, R., Kimsey, M. J., and Page-Dumroese, D. S. (2021). Soil Sustainability and Harvest Operations.
516 *General Technical Report RMRS*. doi: 10.2737/RMRS-GTR-421
517 Curzon, M. T., Slesak, R. A., Palik, B. J., and Schwager, J. K. (2022). Harvest impacts to stand development and soil properties
518 across soil textures: 25-year response of the aspen Lake States LTSP installations. *Forest Ecology and Management* 504,
519 119809. doi: 10.1016/j.foreco.2021.119809
520 D'Acqui, L. P., Certini, G., Cambi, M., and Marchi, E. (2020). Machinery's impact on forest soil porosity. *Journal of*
521 *Terramechanics* 91, 65–71. doi: 10.1016/j.jterra.2020.05.002
522 DeArmond, D., Ferraz, J., and Higuchi, N. (2021). Natural Recovery of Skid Trails. A Review. *Canadian Journal of Forest*
523 *Research*. doi: 10.1139/cjfr-2020-0419
524 Eijkelkamp Agrisearch Equipment (2013). *User Manual for the Moisture Meter type HH2*. Accessed August 07, 2020,
525 https://www.eijkelkamp.com/download.php?file=M1142602e_Soil_moisture_meter_f1ab.pdf
526 Eliasson, L. (2005). Effects of forwarder tyre pressure on rut formation and soil compaction. *Silva Fennica* 39, 549–557. doi:
527 10.14214/sf.366
528 Finnish Meteorological Institute (2023). *Harvester Seasons*. Accessed November 08, 2023,
529 https://harvesterseasons.com/HarvesterSeasons_Description2pager_v2.pdf
530 Francesca, V., Osvaldo, F., Stefano, P., and Paola, R. P. (2010). Soil Moisture Measurements: Comparison of Instrumentation
531 Performances. *J. Irrig. Drain Eng.* 136, 81–89. doi: 10.1061/(ASCE)0733-9437(2010)136:2(81)
532 Grüll, M. (2011). Den Waldboden schonen–Vorsorgender Bodenschutz beim Einsatz von Holzerntetechnik [Soil protection
533 in forest operations]. *Eberswalder Forstliche Schriftenreihe* 47, 37–44.
534 Guo, M., Li, J., Sheng, C., Xu, J., and Wu, L. (2017). A Review of Wetland Remote Sensing. *Sensors (Basel)* 17. doi:
535 10.3390/s17040777
536 Hansson, L., Šimůnek, J., Ring, E., Bishop, K., and Gärdenäs, A. I. (2019). Soil Compaction Effects on Root-Zone Hydrology
537 and Vegetation in Boreal Forest Clearcuts. *Soil Sci. Soc. Am. j.* 83, 239. doi: 10.2136/sssaj2018.08.0302
538 Hauglin, M., Rahlf, J., Schumacher, J., Astrup, R., and Breidenbach, J. (2021). Large scale mapping of forest attributes using
539 heterogeneous sets of airborne laser scanning and National Forest Inventory data. *Forest Ecosystems* 8, 65. doi:
540 10.1186/s40663-021-00338-4
541 Heppelmann, J. B., Talbot, B., Antón Fernández, C., and Astrup, R. (2022). Depth-to-water maps as predictors of rut severity
542 in fully mechanized harvesting operations. *International Journal of Forest Engineering* 33, 108–118. doi:
543 10.1080/14942119.2022.2044724
544 Heubaum, F. (2015). *Bodenschutz im Staatsbetrieb Sachsenforst [Soil protection]: Projekte zur Technologieerprobung*.
545 Accessed November 05, 2021, https://www.sbs.sachsen.de/download/Bodenschutz_Projekte_2015_09_30.pdf
546 Hijmans, R. J. (2020). raster: Geographic Data Analysis and Modeling, https://CRAN.R-project.org/package=raster
547 Hillel, D. (1998). *Environmental soil physics: Fundamentals, applications, and environmental considerations*. San Diego,
548 California: Elsevier.
549 Hoffmann, S., Schönauer, M., Heppelmann, J., Asikainen, A., Cacot, E., Eberhard, B., et al. (2022). Trafficability Prediction
550 Using Depth-to-Water Maps: the Status of Application in Northern and Central European Forestry. *Curr Forestry Rep* 338,

124. doi: 10.1007/s40725-021-00153-8

Horn, R., Vossbrink, J., Peth, S., and Becker, S. (2007). Impact of modern forest vehicles on soil physical properties. *Forest Ecology and Management* 248, 56–63. doi: 10.1016/j.foreco.2007.02.037

James, S. E., Pärtel, M., Wilson, S. D., and Peltzer, D. A. (2003). Temporal heterogeneity of soil moisture in grassland and forest. *Journal of Ecology*, 234–239.

Jones, M.-F., and Arp, P. (2017). Relating Cone Penetration and Rutting Resistance to Variations in Forest Soil Properties and Daily Moisture Fluctuations. *Open Journal of Soil Science* 07, 149–171. doi: 10.4236/ojss.2017.77012

Jones, M.-F., and Arp, P. (2019). Soil Trafficability Forecasting. *Open Journal of Forestry* 9, 296–322. doi: 10.4236/ojf.2019.94017

Kelliher, F. M., Leuning, R., and Schulze, E. D. (1993). Evaporation and canopy characteristics of coniferous forests and grasslands. *Oecologia* 95, 153–163. doi: 10.1007/BF00323485

Kemppinen, J., Niittynen, P., Riihimäki, H., and Luoto, M. (2018). Modelling soil moisture in a high-latitude landscape using LiDAR and soil data. *Earth Surf. Process. Landforms* 43, 1019–1031. doi: 10.1002/esp.4301

Koen Hufkens, Reto Stauffer, and Elio Campitelli (2019). *khufkens/ecmwfr: ecmwfr*. Zenodo.

Kristensen, J. A., Balstrøm, T., Jones, R. J. A., Jones, A., Montanarella, L., Panagos, P., et al. (2019). Development of a harmonised soil profile analytical database for Europe: a resource for supporting regional soil management. *SOIL* 5, 289–301. doi: 10.5194/soil-5-289-2019

Kuglerová, L., Hasselquist, E. M., Richardson, J. S., Sponseller, R. A., Kreutzweiser, D. P., and Laudon, H. (2017). Management perspectives on Aqua incognita : Connectivity and cumulative effects of small natural and artificial streams in boreal forests. *Hydrological Processes* 31, 4238–4244. doi: 10.1002/hyp.11281

Kuhn, M. (2020). *caret: Classification and Regression Training*. Accessed November 09, 2021, https://CRAN.R-project.org/package=caret

Kursa, M. B., and Rudnicki, W. R. (2010). Feature Selection with the Boruta Package. *J. Stat. Soft.* 36. doi: 10.18637/jss.v036.i11

Labelle, E. R., and Jaeger, D. (2018). Management Implications of Using Brush Mats for Soil Protection on Machine Operating Trails during Mechanized Cut-to-Length Forest Operations. *Forests* 10, 19. doi: 10.3390/f10010019

Labelle, E. R., Poltorak, B. J., and Jaeger, D. (2019). The role of brush mats in mitigating machine-induced soil disturbances: An assessment using absolute and relative soil bulk density and penetration resistance. *Canadian Journal of Forest Research* 49, 164–178. doi: 10.1139/cjfr-2018-0324

Lal, P., Singh, G., Das, N. N., Colliander, A., and Entekhabi, D. (2022). Assessment of ERA5-Land Volumetric Soil Water Layer Product Using In Situ and SMAP Soil Moisture Observations. *IEEE Geosci. Remote Sensing Lett.* 19, 1–5. doi: 10.1109/LGRS.2022.3223985

Larson, J., Lidberg, W., Ågren, A. M., and Laudon, H. (2022). *Predicting soil moisture conditions across a heterogeneous boreal catchment using terrain indices*.

Leach, J. A., Lidberg, W., Kuglerová, L., Peralta-Tapia, A., Ågren, A., and Laudon, H. (2017). Evaluating topography-based predictions of shallow lateral groundwater discharge zones for a boreal lake-stream system. *Water Resources Research* 53, 5420–5437. doi: 10.1002/2016WR019804

Lidberg, W., Nilsson, M., and Ågren, A. (2020). Using machine learning to generate high-resolution wet area maps for

589 planning forest management: A study in a boreal forest landscape. *Ambio* 49, 475–486. doi: 10.1007/s13280-019-01196-9
590 Mattila, U., and Tokola, T. (2019). Terrain mobility estimation using TWI and airborne gamma-ray data. *Journal of*
591 *environmental management* 232, 531–536. doi: 10.1016/j.jenvman.2018.11.081
592 McNabb, D. H., Startsev, A. D., and Nguyen, H. (2001). Soil Wetness and Traffic Level Effects on Bulk Density and Air-
593 Filled Porosity of Compacted Boreal Forest Soils. *Soil Science Society of America Journal* 65, 1238–1247. doi:
594 10.2136/sssaj2001.6541238x
595 Mohtashami, S., Eliasson, L., Jansson, G., and Sonesson, J. (2017). Influence of soil type, cartographic depth-to-water, road
596 reinforcement and traffic intensity on rut formation in logging operations: a survey study in Sweden. *Silva Fennica* 51. doi:
597 10.14214/sf.2018
598 Moore, I. D., Grayson, R. B., and Ladson, A. R. (1991). Digital terrain modelling: A review of hydrological,
599 geomorphological, and biological applications. *Hydrol. Process.* 5, 3–30. doi: 10.1002/hyp.3360050103
600 Muñoz-Sabater, J., Dutra, E., Agustí-Panareda, A., Albergel, C., Arduini, G., Balsamo, G., et al. (2021). ERA5-Land: a state-
601 of-the-art global reanalysis dataset for land applications. *Earth Syst. Sci. Data* 13, 4349–4383. doi: 10.5194/essd-13-4349-
602 2021
603 Murphy, P. N. C., Ogilvie, J., and Arp, P. (2009). Topographic modelling of soil moisture conditions: A comparison and
604 verification of two models. *European Journal of Soil Science* 60, 94–109. doi: 10.1111/j.1365-2389.2008.01094.x
605 Murphy, P. N. C., Ogilvie, J., Connor, K., and Arp, P. (2007). Mapping wetlands: A comparison of two different approaches
606 for New Brunswick, Canada. *WETLANDS* 27, 846–854. doi: 10.1672/0277-5212(2007)27[846:MWACOT]2.0.CO;2
607 Murphy, P. N. C., Ogilvie, J., Meng, F.-R., White, B., Bhatti, J. S., and Arp, P. (2011). Modelling and mapping topographic
608 variations in forest soils at high resolution: A case study. *Ecological Modelling* 222, 2314–2332. doi:
609 10.1016/j.ecolmodel.2011.01.003
610 Oliveira, V. A., Rodrigues, A. F., Morais, M. A. V., Terra, M. d. C. N. S., Guo, L., and Mello, C. R. (2021). Spatiotemporal
611 modelling of soil moisture in an A tlantic forest through machine learning algorithms. *Eur J Soil Sci* 72, 1969–1987. doi:
612 10.1111/ejss.13123
613 Picchio, R., Latterini, F., Mederski, P. S., Tocci, D., Venanzi, R., Stefanoni, W., et al. (2020). Applications of GIS-Based
614 Software to Improve the Sustainability of a Forwarding Operation in Central Italy. *Sustainability* 12, 5716. doi:
615 10.3390/su12145716
616 Poltorak, B. J., Labelle, E. R., and Jaeger, D. (2018). Soil displacement during ground-based mechanized forest operations
617 using mixed-wood brush mats. *Soil and Tillage Research* 179, 96–104. doi: 10.1016/j.still.2018.02.005
618 Quinn, P., Beven, K., Chevallier, P., and Planchon, O. (1991). The prediction of hillslope flow paths for distributed
619 hydrological modelling using digital terrain models. *Hydrol. Process.* 5, 59–79. doi: 10.1002/hyp.3360050106
620 R Core Team (2023). *R: A Language and Environment for Statistical Computing*. Vienna, Austria: The R Foundation for
621 Statistical Computing.
622 Ring, E., Ågren, A., Bergkvist, I., Finér, L., Johansson, F., and Högbom, L. (2022). *A guide to using wet area maps in forestry:*
623 *En guide för hur man kan använda markfuktighetskartor i skogsbruket*. ARBETSRAPPORT 1051-2020. Uppsala, Sweden.
624 Schönauer, M., Hoffmann, S., Maack, J., Jansen, M., and Jaeger, D. (2021a). Comparison of Selected Terramechanical Test
625 Procedures and Cartographic Indices to Predict Rutting Caused by Machine Traffic during a Cut-to-Length Thinning
626 Operation. *Forests* 12, 113. doi: 10.3390/f12020113

627 Schönauer, M., and Maack, J. (2021). R-code for calculating depth-to-water (DTW) maps using GRASS GIS (Version v1).
628 *Zenodo*. doi: 10.5281/zenodo.5638518
629 Schönauer, M., Prinz, R., Väätäinen, K., Astrup, R., Pszenny, D., Lindeman, H., et al. (2022). Spatio-temporal prediction of
630 soil moisture using soil maps, topographic indices and SMAP retrievals. *International Journal of Applied Earth*
631 *Observation and Geoinformation* 108, 102730. doi: 10.1016/j.jag.2022.102730
632 Schönauer, M., Väätäinen, K., Prinz, R., Lindeman, H., Pszenny, D., Jansen, M., et al. (2021b). Spatio-temporal prediction
633 of soil moisture and soil strength by depth-to-water maps. *International Journal of Applied Earth Observation and*
634 *Geoinformation* 105, 102614. doi: 10.1016/j.jag.2021.102614
635 Sirén, M., Salmivaara, A., Ala-Ilomäki, J., Launiainen, S., Lindeman, H., Uusitalo, J., et al. (2019). Predicting forwarder rut
636 formation on fine-grained mineral soils. *Scandinavian Journal of Forest Research* 34, 145–154. doi:
637 10.1080/02827581.2018.1562567
638 Sørensen, R., and Seibert, J. (2007). Effects of DEM resolution on the calculation of topographical indices: TWI and its
639 components. *Journal of Hydrology* 347, 79–89. doi: 10.1016/j.jhydrol.2007.09.001
640 Suvinen, A., and Saarilahti, M. (2006). Measuring the mobility parameters of forwarders using GPS and CAN bus techniques.
641 *Journal of Terramechanics* 43, 237–252. doi: 10.1016/j.jterra.2005.12.005
642 Tromp-van Meerveld, H. J., and McDonnell, J. J. (2006). On the interrelations between topography, soil depth, soil moisture,
643 transpiration rates and species distribution at the hillslope scale. *Advances in Water Resources* 29, 293–310. doi:
644 10.1016/j.advwatres.2005.02.016
645 Uusitalo, J., Ala-Ilomäki, J., Lindeman, H., Toivio, J., and Sirén, M. (2019). Modelling soil moisture – soil strength
646 relationship of fine-grained upland forest soils. *Silva Fennica* 53. doi: 10.14214/sf.10050
647 Uusitalo, J., Ala-Ilomäki, J., Lindeman, H., Toivio, J., and Sirén, M. (2020). Predicting rut depth induced by an 8-wheeled
648 forwarder in fine-grained boreal forest soils. *Annals of forest science* 77. doi: 10.1007/s13595-020-00948-y
649 Vega-Nieva, D. J., Murphy, P. N. C., Castonguay, M., Ogilvie, J., and Arp, P. (2009). A modular terrain model for daily
650 variations in machine-specific forest soil trafficability. *Canadian Journal of Soil Science* 89, 93–109. doi:
651 10.4141/CJSS06033
652 Walker, J. P., Willgoose, G. R., and Kalma, J. D. (2004). In situ measurement of soil moisture: a comparison of techniques.
653 *Journal of Hydrology* 293, 85–99. doi: 10.1016/j.jhydrol.2004.01.008
654 White, B., Ogilvie, J., Campbell, D. M.H., Hiltz, D., Gauthier, B., Chisholm, H. K., et al. (2012). Using the Cartographic
655 Depth-to-Water Index to Locate Small Streams and Associated Wet Areas across Landscapes. *Canadian Water Resources*
656 *Journal* 37, 333–347. doi: 10.4296/cwrj2011-909
657 Wright, M. N., and Ziegler, A. (2017). ranger: A Fast Implementation of Random Forests for High Dimensional Data in C++
658 and R. *J. Stat. Soft.* 77. doi: 10.18637/jss.v077.i01
659